

The Rice Pentatricopeptide Repeat Protein RF5 Restores Fertility in Hong-Lian Cytoplasmic Male-Sterile Lines via a Complex with the Glycine-Rich Protein GRP162[©]^W

Jun Hu,^{a,b,c} Kun Wang,^{a,b,c} Wenchao Huang,^{a,b,c} Gai Liu,^a Ya Gao,^a Jianming Wang,^a Qi Huang,^{a,b} Yanxiao Ji,^{a,b} Xiaojian Qin,^{a,b} Lei Wan,^{a,b} Renshan Zhu,^{a,b,c} Shaoqing Li,^{a,b,c} Daichang Yang,^{a,b,c} and Yingguo Zhu^{a,b,c,1}

^aKey Laboratory of the Ministry of Education for Plant Developmental Biology, College of Life Sciences, Wuhan University, Wuhan 430072, China

^bEngineering Research Center for Plant Biotechnology and Germplasm Utilization, Ministry of Education, Wuhan University, Wuhan 430072, China

^cState Key Laboratory for Hybrid Rice, College of Life Sciences, Wuhan University, Wuhan 430072, China

The cytoplasmic male sterility (CMS) phenotype in plants can be reversed by the action of nuclear-encoded fertility restorer (*Rf*) genes. The molecular mechanism involved in *Rf* gene-mediated processing of CMS-associated transcripts is unclear, as are the identities of other proteins that may be involved in the CMS-*Rf* interaction. In this study, we cloned the restorer gene *Rf5* for Hong-Lian CMS in rice and studied its fertility restoration mechanism with respect to the processing of the CMS-associated transcript *atp6-orfH79*. RF5, a pentatricopeptide repeat (PPR) protein, was unable to bind to this CMS-associated transcript; however, a partner protein of RF5 (GRP162, a Gly-rich protein encoding 162 amino acids) was identified to bind to *atp6-orfH79*. GRP162 was found to physically interact with RF5 and to bind to *atp6-orfH79* via an RNA recognition motif. Furthermore, we found that RF5 and GRP162 are both components of a restoration of fertility complex (RFC) that is 400 to 500 kD in size and can cleave CMS-associated transcripts *in vitro*. Evidence that a PPR protein interacts directly with a Gly-rich protein to form a subunit of the RFC provides a new perspective on the molecular mechanisms underlying fertility restoration.

INTRODUCTION

Cytoplasmic male sterility (CMS), a maternally inherited inability to produce functional pollen, has been observed in more than 200 species of higher plants. At the molecular level, CMS is correlated with aberrant, often chimeric, mitochondrial genes in all cases that have been examined (Hanson and Bentolila, 2004; Chase, 2007). The CMS phenotype can be rescued by a class of nuclear genes termed restorer of fertility (*Rf*) genes. In general, *Rf* genes belong to a large, well-defined family of genes that encode organelle-targeted pentatricopeptide repeat (PPR) proteins. Notable exceptions include maize (*Zea mays*) *Rf2*, which encodes an aldehyde dehydrogenase that accumulates in mitochondria (Cui et al., 1996), *Rf17* for CW-CMS rice (*Oryza sativa*; Fujii and Toriyama, 2009), and the *Rf2* gene for Lead type-CMS (LD-CMS) in rice, a Gly-rich protein (GRP) (Itabashi et al., 2011). *Rf* genes encoding PPR proteins include *PPR592* in petunia (*Petunia hybrida*), *Rf1k* in Kosenia rapeseed, *Rfo* in radish (*Raphanus*

sativus), *PPR13* in sorghum (*Sorghum bicolor*), and *Rf1a/Rf1b* in Boro II type CMS (BT-CMS) rice (Bentolila et al., 2002; Brown et al., 2003; Desloire et al., 2003; Kazama and Toriyama, 2003; Koizuka et al., 2003; Akagi et al., 2004; Komori et al., 2004; Klein et al., 2005; Wang et al., 2006). *Rf* genes act to reduce the accumulation of CMS-associated RNAs and/or proteins in F1 hybrids.

PPR proteins can be subdivided into two families (P and PLS) based on the structure of the PPR motif (Schmitz-Linneweber and Small, 2008). Several nuclear-encoded PPR proteins of the PLS family exhibit RNA binding activity (Schmitz-Linneweber et al., 2005; Beick et al., 2008; Pfalz et al., 2009) or RNA editing activity (Kotera et al., 2005; Okuda et al., 2006; Shikanai, 2006; Robbins et al., 2009) and contain an E motif and/or a DYW motif essential for RNA binding and/or editing. It has been postulated that the E/DYW motif may be an as yet unknown enzyme (Salone et al., 2007; Okuda et al., 2009). However, most RF-related PPR proteins belong to the P subclass, which lacks the E/DYW motif (except PPR13 in sorghum), and most P subclass PPR proteins have so far been shown to lack catalytic sites for RNA binding or editing. Accordingly, it is possible that partner proteins associated with the PPR-RNA complex could perform the RNA processing steps. Thus, at the molecular level, it remains unclear how RF proteins that contain PPR motifs process chimeric RNAs in CMS lines.

Hong-Lian (HL) CMS rice was bred by backcrossing red-awned wild rice (*Oryza rufipogon*) with the *indica* variety Lian Tang-Zao in the 1970s. HL-CMS, which is similar to BT-CMS,

¹ Address correspondence to zhuyg@public.wh.hb.cn.

The author responsible for distribution of materials integral to the findings presented in this article in accordance with the policy described in the Instructions for Authors (www.plantcell.org) is: Yingguo Zhu (zhuyg@public.wh.hb.cn).

[©]Some figures in this article are displayed in color online but in black and white in the print edition.

^WOnline version contains Web-only data.

www.plantcell.org/cgi/doi/10.1105/tpc.111.093211

belongs to a gametophytic CMS group that exhibits pollen abortion at the bicellular stage, whereas BT-CMS pollen aborts at the tricellular stage. The HL-type hybrid has been widely adopted and was planted on nearly four million hectares in China and southeast Asia in the last two decades, contributing greatly to the food security of the world. Previous work has shown that *atp6-orfH79* is the CMS-associated HL-CMS transcript, and there is only one copy of *atp6-orfH79* in the mitochondrial genome. The sequences of *orfH79* from HL-CMS and *orf79* from BT-CMS share 98% identity but show significant divergence in the intergenic region connecting them to *atp6* (Yi et al., 2002; Peng et al., 2010). Comparison of the restoration process in BT-CMS and HL-CMS has shown that the CMS-RNA, *atp6-orf79* or *atp6-orfH79*, can be cleaved to *atp6* plus either *orf79* or *orfH79* in the presence of *Rf1* or *Rf5*, respectively. A previous report suggested that RF1 can bind directly to the CMS-RNA *atp6-orf79* (Kazama et al., 2008). RF1A cleaves the *atp6-orf79* transcript, and RF1B promotes its degradation (Wang et al., 2006), suggesting two distinct pathways for restoration. In the case of HL-CMS, fertility can be independently restored by either of two genes, *Rf5* or *Rf6* (Liu et al., 2004), although the mechanisms underlying CMS and fertility restoration have not been defined.

Here, we report the cloning of the *Rf5* gene, which encodes a PPR protein, and we show that *Rf5* is identical to *Rf1* (*Rf1a*) in BT-CMS rice. We find that the fertility restoration function of RF5 requires GRP162, which recruits the substrate for the RF complex (RFC) by binding to CMS-associated transcripts. Our data suggest that GRP162 plays a critical role in the CMS/*Rf* system.

RESULTS

Identification of *Rf5* as a PPR Protein by Map-Based Cloning

Rf5 was mapped to chromosome 10 between the RM1108 and RM5373 markers (Liu et al., 2004). A BC₃F₁ population of 1979 individuals was used for the fine mapping of *Rf5*. An additional 27 simple sequence repeat (SSR) markers were used for mapping, and the *Rf5* locus was narrowed down to the ~67-kb region flanked by the RM6469 and RM25659 markers (Figure 1A). A search of the rice genome sequence database (www.gramene.org) revealed that a BAC clone, OSJNBa0017E08 BAC, covers these two SSR markers. The OSJNBa0017E08 BAC was used as a probe to isolate an *Rf5*-containing BAC from the *Rf5* line Milyang32. A positive BAC clone, 68F6, was obtained by screening a Milyang23 BAC library and was subcloned into pUC18/*Sall* for sequencing. BLAST analysis of the BAC sequence revealed that it contained three genes belonging to the PPR family: *PPR791*, *PPR683*, and *PPR794*. These candidate genes were isolated, individually ligated into the pCAMBIA1301-UBI vector containing the ubiquitin promoter, and introduced into the *rf5* HL-CMS line YueTai A (YTA) for genetic complementation tests. If the introduced construct can complement the *rf5* mutation in YTA, the transgenic plants should produce viable pollen and therefore should be male fertile. The fertility of independent transformants containing the individual candidate genes was assayed by staining pollen with 1% I₂-KI (see Supplemental Table 1 online). All eight of the T0 plants from the *PPR791*

transformation showed the expected fertile phenotype, whereas all 17, 10, and 9 of the T0 plants derived from *PPR683*, *PPR794*, and the empty vector were male sterile, indicating that these constructs failed to complement the *rf5* mutation in YTA. To genetically confirm the fertility restoration phenotype of *PPR791*, three independent T0 transgenic plants were self-bred and test-crossed with YTA. In the progeny of the self-cross, a 1:1 genetic segregation ratio was observed in 38 T1 progeny, with 20 plants producing 93.76% fertile pollen and 18 producing 49.69% fertile pollen, which is the expected gametophytic genetic segregation ($\chi^2 = 0.013$ for 1:1, $P < 0.05$; Figures 1B and 1C; see Supplemental Table 2 online). These results indicate that *PPR791* is the functional open reading frame (ORF) of *Rf5*. *PPR791* has been identified as both *Rf1* and *Rf1a* in previous studies (Akagi et al., 2004; Komori et al., 2004; Wang et al., 2006).

In addition to testing the fertility phenotype, we also determined whether the complementation construct affected the cleavage of the CMS-associated transcript, *atp6-orfH79*. An RNA gel blot assay with *orfH79* as a probe showed that *atp6-orfH79* is cleaved in the presence of *Rf5* in the leaves of transgenic T1 line seedlings and in the near-isogenic line (NIL) F1 progeny (Figure 1E). PCR with *HptII*-specific primers was used to verify the segregation of the transgenic copy of *PPR791* in the F1 progeny (Figure 1E), and the PCR results were consistent with the phenotypes of these progeny, confirming the functional complementation of *Rf5* in 53 F1 progeny of the test crosses (see Supplemental Table 3 online). Therefore, we concluded that *PPR791* corresponds to the *Rf5* locus identified in the HL-CMS system.

To characterize the allele of *Rf5* present in the CMS line, *PPR791* was sequenced from the YTA genome. A single-nucleotide T-to-A mutation was found at position 912 (see Supplemental Figure 1 online). This single-nucleotide polymorphism causes a codon change from TAT to TAA in the fourth PPR domain, resulting in a truncated PPR protein in the YTA line. These data further confirm *PPR791* as the *Rf5* product.

RF5 Cannot Bind Directly to the *atp6-orfH79* Transcript in Vitro

Following the map-based cloning of *Rf5*, we investigated the mechanism by which RF5 processes the CMS-associated transcript *atp6-orfH79* (see Supplemental Figure 2 online). Electrophoretic mobility shift assays (EMSAs) were performed to test whether RF5 interacts with *atp6-orfH79* transcripts directly. Eighty-one amino acids were removed from the N terminus of RF5 to permit its fusion to a Maltose Binding Protein (MBP) tag and allow the protein's expression to be monitored. The MBP-RF5 fusion protein expressed in *Escherichia coli* was soluble (see Supplemental Figure 3A online), and it was purified to enable quadrupole-time of flight mass spectrum sequencing and circular dichroism analysis to confirm its proper synthesis and folding. The quadrupole-time of flight mass spectrum results confirmed that the expressed protein was composed exclusively of the MBP tag and RF5 twice (see Supplemental Figure 3B online). The circular dichroism analysis revealed that the recombinant protein was composed of 46.7% α -helix and 17.6% turn-sheet (see Supplemental Figure 3C online). Comparison with the folding

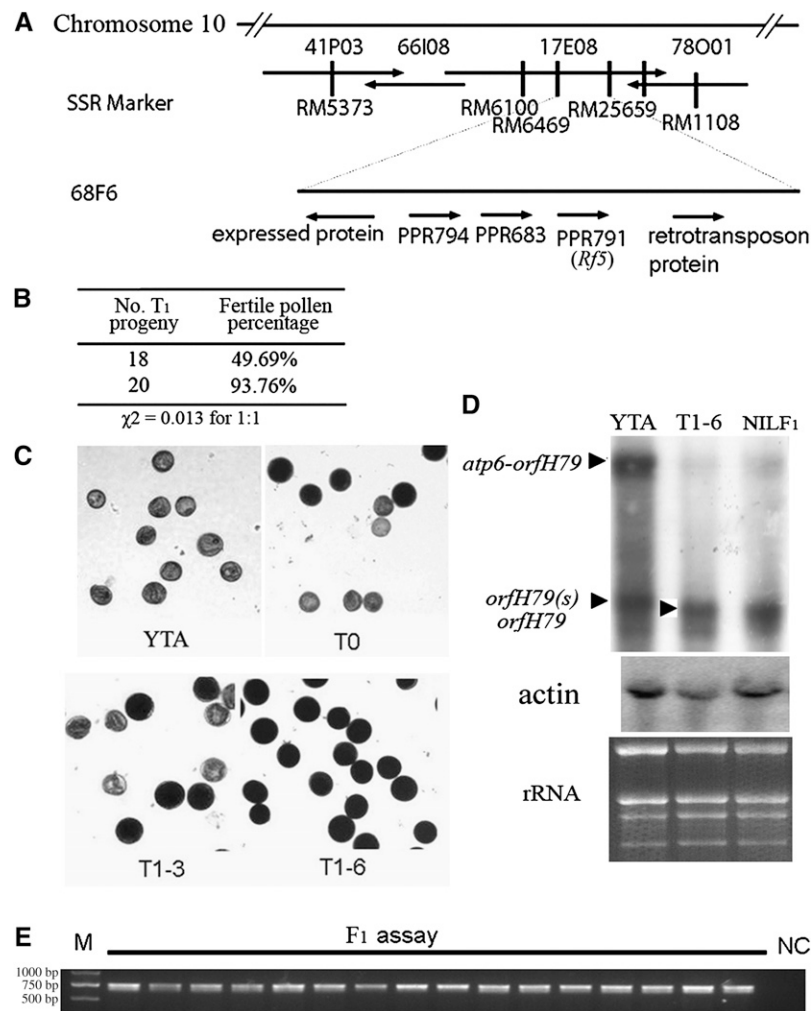


Figure 1. Map-Based Cloning of *Rf5*.

(A) The *Rf5* locus was initially mapped to chromosome 10 between the SSR markers RM1108 and RM5373 and subsequently narrowed down to a 67-kb interval between the markers RM6469 and RM25659. Subcloning and sequencing of Milyang23 BAC clone 68F6.

(B) Analysis of the percentage of fertile pollen from T1 progeny of the *rf5* line YTA containing the transgenic *Rf5* complementation construct ($\chi^2 = 0.013$ for 1:1, $P < 0.05$).

(C) Pollen fertility was assessed by 1% I_2 -KI staining. Darkly stained pollen is fertile, and lightly stained pollen is sterile.

(D) RNA gel blot analysis of the CMS *rf5* line YTA, the *Rf5* transgenic YTA lines T₁₋₆, and the *Rf5* line NILF₁ using *orfH79* as a probe and an actin probe as a control; an ethidium bromide stain of the gel is shown to confirm equal RNA loading. The RNA was extracted from seedling leaves.

(E) *HptII* gene in the transgenic vector was amplified and the PCR products were loaded on a 1.5% agarose gel to show the cosegregation of the *HptII* site and fertile plants among F1 progeny. M, marker DL2000, NC, negative control.

predicted by the SOPMA software (<http://npsa-pbil.ibcp.fr/>) of 54.2% α -helix and 11.1% turn-sheet forms suggests that the expressed protein is correctly folded.

The MBP-RF5 protein was used in EMSAs to test its binding to *atp6-orfH79* RNA. The results indicated that RF5 does not bind *atp6-orfH79* mRNA in vitro (Figure 2A). To test the possibility of MBP interference in binding, we also removed the MBP tag and again obtained negative results for RF5 RNA binding activity.

To further explore whether RF5 directly binds to *atp6-orfH79* mRNA, three overlapping ~ 90 -nucleotide RNAs (designated A,

B, and C) spanning the *atp6-orfH79* intragenic region were used in a yeast three-hybrid assay (Figure 2B). No interaction was observed between RF5 and these intragenic fragments (see Supplemental Figure 4A online). The lack of interaction was further confirmed by measuring β -galactosidase activity via standard filter assays with X-Gal (see Supplemental Figure 4B online). Therefore, we conclude that RF5 does not bind to *atp6-orfH79* mRNA, implying that the fertility restoration function of RF5 requires other RNA binding proteins that process *atp6-orfH79* mRNA.

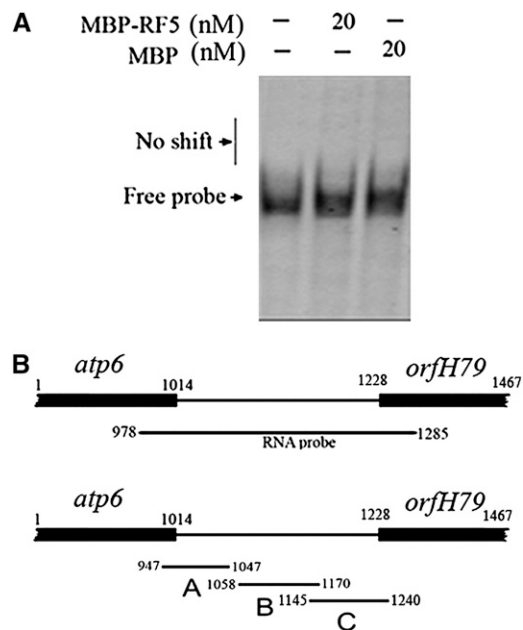


Figure 2. Interaction between RF5 and CMS-Associated Transcripts.

(A) EMSA with MBP-RF5 and MBP tag using the *atp6-orfH79* RNA probe.

(B) The *atp6-orfH79* intragenic region from 978 to 1285 nucleotides, including parts of the *atp6* and *orfH79* sequences, was in vitro transcribed as a CMS RNA probe for EMSA. The intragenic region including parts of the *atp6* and *orfH79* sequences was divided into three parts, A, B, and C, for a yeast three-hybrid assay.

A GRP Interacts with RF5

To search for an RF5 interaction partner, we constructed a bacterial two-hybrid library of 1.03×10^6 clones averaging 1.1 kb in length from cDNA derived from an F1 hybrid spikelet (see Supplemental Figure 5 online). A pBT-RF5 construct was used as bait to screen the library, and 13 clones were obtained by stringent selection on dual selective medium plates. Sequencing of these clones revealed eight different proteins as potential RF5 interactors (see Supplemental Table 4 online). Bioinformatic analysis of the resulting protein candidates showed one GRP containing an RNA recognition motif (RRM) that is involved in RNA binding activity. Previous studies have suggested that the GRP family is essential for plant development (Vermel et al., 2002; Maris et al., 2005; Dollins et al., 2007). Thus, GRP162 (Os12 g0632000) was selected as a candidate for further study.

The yeast two-hybrid system was used to validate the interaction between GRP162 and RF5. Two constructs, pGBKT7-RF5 (as bait) and pGADT7-GRP162 (as prey), were created and cotransformed into the yeast strain AH109. The interaction between GRP162 and RF5 was revealed when the transformant colonies grew on medium containing SD/-Leu/-Trp/-His/-Ade, whereas no interaction was found between either pGBKT7-RF5 and pGADT7 or pGBKT7 and pGADT7-GRP162 (Figure 3A).

We also examined the interaction of RF5 with GRP162 using an affinity column assay in which His-tagged GRP162 was conju-

gated to a HisTrap column and recombinant MBP-RF5 was applied to the column. The column was washed and fractions were eluted; the eluted fractions were analyzed by SDS-PAGE and stained with Coomassie blue. We found that His-GRP and MBP-RF5 both eluted with the same profile, with maximal elution in fraction 9 (Figure 3B). Fraction 9 was further confirmed by immunoblotting with anti-His and anti-MBP antibodies. Negative controls were used to confirm that GRP162 did not bind to the MBP-tag, and RF5 did not bind to the His-tag (Figure 3C). These results demonstrated that GRP162 interacts with RF5 in vitro.

Bimolecular fluorescence complementation (BiFC) assays were next used to further test the interaction between GRP162 and RF5. RF5 and GRP162 were fused to the inactive N-terminal and C-terminal fragments (pSPYNE and pSPYCE, respectively) of yellow fluorescent protein (YFP). Strong fluorescence was observed when the RF5 and GRP162 fusions were coexpressed in onion epidermal cells (Figure 3D), whereas no fluorescence was detected in the negative control, indicating that the two proteins physically interact in vivo. Furthermore, fluorescence was observed upon cotransformation of GRP162-YFP(N) with GRP162-YFP(C), whereas no fluorescence was observed in cells cotransformed with RF5-YFP(N) and RF5-YFP(C). These results suggested that GRP162 may form a homodimer in vivo (Figure 3E). We also tested whether the GRP-RF5 heterodimer or the GRP homodimer localized to mitochondria, as would be expected if it acts on a mitochondrial RNA, by staining with MitoTracker Red. Although GRP162 homodimers did not overlap with mitochondria, some of the RF5-GRP162 heterodimers did localize to mitochondria (Figures 3D and 3E). These data suggest that the interaction of RF5 with GRP162 changes the localization of GRP162. In the National Center for Biotechnology Information (NCBI) database, the GRP162 sequence showed that the sequence from 81 to 82 amino acids may be a dimerization site. Taken together, these results provide compelling evidence that GRP162 interacts with RF5 both in vitro and in vivo and that GRP162 may also form a homodimer.

GRP162 Accumulates in Mitochondria in the Presence of RF5

A comparison of GRP162 sequences in the restorer line NILF₁ and the CMS line YTA revealed no exonic differences. We then evaluated the expression of the *GRP162* gene in anthers by quantitative RT-PCR, comparing lines YTA and NILF₁. The expression of GRP162 was found to be ~2.25 times higher in the *Rf5* restorer line NILF₁ than in YTA (see Supplemental Figure 6 online). We next used subcellular fractionation and immunoblot analysis to examine the subcellular localization GRP162 in the restorer and CMS lines. GRP162 was detected in the mitochondria of an F1 hybrid plant, but GRP162 was not detected in the mitochondria of the YTA line (Figure 4). Previous studies showed that RF5 has a mitochondrial targeting presequence (Wang et al., 2006), but analysis of the GRP162 sequence produced no evidence of a mitochondrial targeting presequence, suggesting diffuse cellular distribution, which is consistent with the results of the BiFC subcellular localization (Figure 3E). The BiFC data also indicated that the subcellular localization of GRP162 changed when it was cotransformed with RF5. These observations

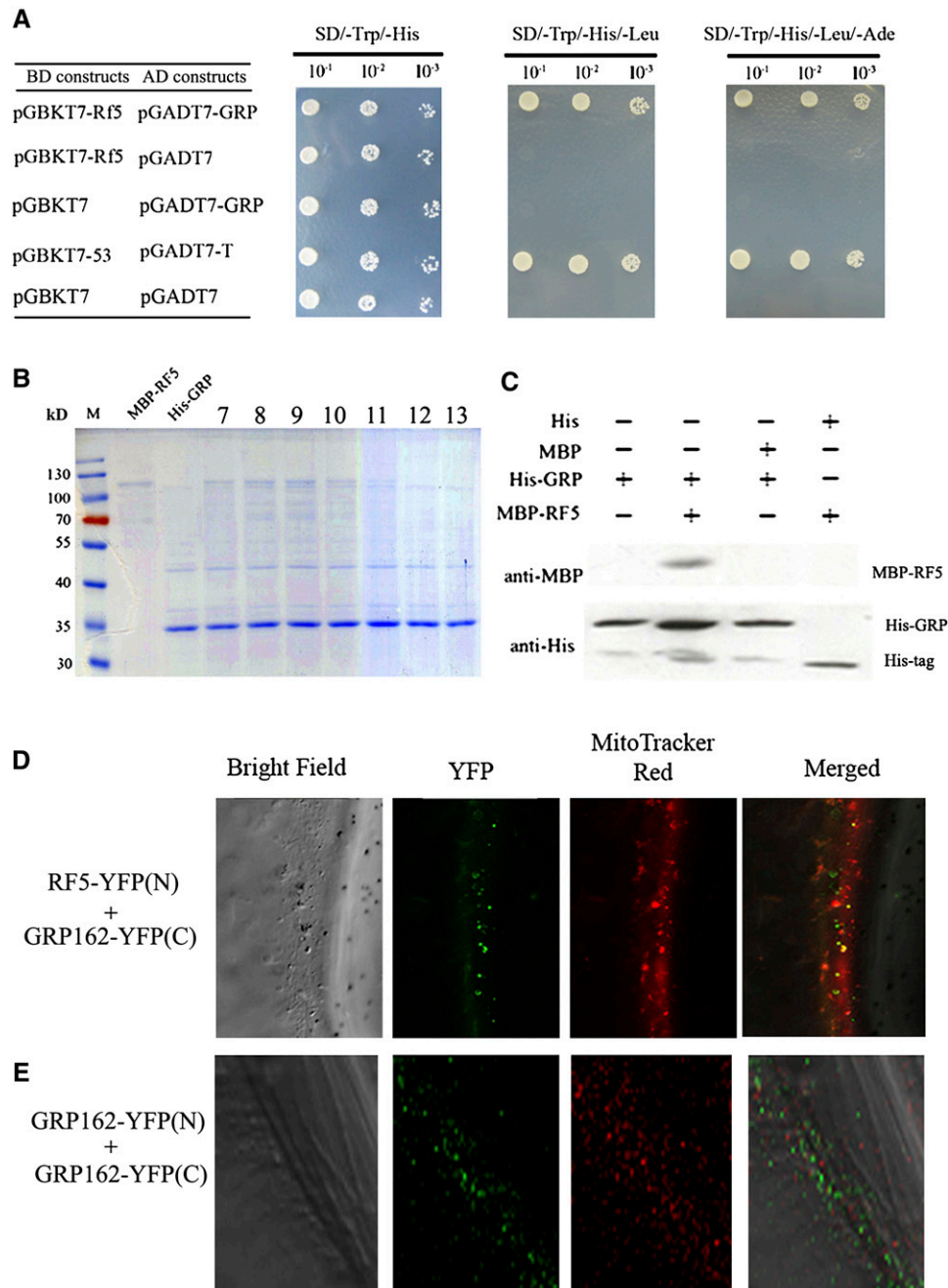


Figure 3. Interaction between GRP162 and RF5.

(A) GRP162 and RF5 were fused to AD and BD vectors, respectively, in a yeast two-hybrid assay to show the interaction between GRP162 and RF5. **(B)** His-tagged GRP162 was conjugated to a HisTrap column, and recombinant MBP-RF5 was applied to the column. The eluted fractions 7 to 13 were loaded into lanes 4 to 10 of SDS-PAGE and visualized with Coomassie blue staining. M, prestained marker 0671 (Fermentas). **(C)** Anti-His and anti-MBP immunoblots of elution fraction 9 from the pull-down assay and controls. **(D)** BiFC assay for detecting molecular interactions between RF5-YFP(N) and GRP162-YFP(C). **(E)** BiFC assay for detecting interactions between GRP162 molecules. GRP162-YFP(N) and GRP162-YFP(C) were coexpressed in onion epidermal cells.

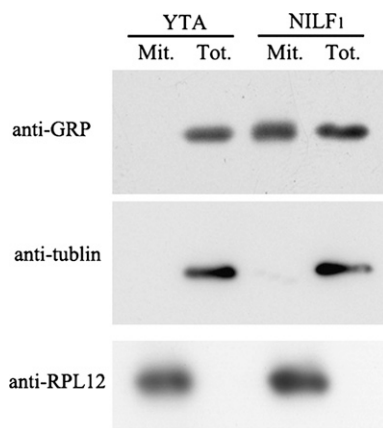


Figure 4. The Expression of GRP162.

Immunodetection of GRP162 accumulation in mitochondria with an anti-GRP162 antibody. An antibody against RPL12, a ribosomal protein cell that is associated with mitochondria, was used as a control. An anti-tubulin antibody was used as a control to rule out contamination. Twenty micrograms of prepared mitochondria (Mit.) cell and 30 μ g of total cell protein (Tot.) from YTA and NILF₁ were loaded.

suggest that RF5 localizes to mitochondria via a targeting presequence and that GRP162 addresses to mitochondria in the presence of the RF5 protein.

CMS-Associated Transcripts Are Captured by GRP162

Bioinformatic analysis revealed that GRP162 contains an RRM motif, prompting us to test whether GRP162 binds to *atp6-orfH79* mRNA to coordinate its processing by RF5. To test this hypothesis, we used EMSA, the yeast three-hybrid system, and coimmunoprecipitation approaches to investigate *atp6-orfH79* mRNA processing. Full-length GRP162 fused with a His-tag was expressed in *E. coli* and purified with a HisTrap FF column (see Supplemental Figure 7 online). In the EMSA assay, His-GRP162 showed a mobility shift when incubated with the *atp6-orfH79* RNA probe (diagrammed in Figure 2D), but no shift was observed when the His-tag alone was incubated with the RNA (Figure 5A). The same gel shift results were obtained when the His-tagged RRM domain alone was incubated with the RNA probe, indicating an interaction between the RRM and *atp6-orfH79* mRNA (Figure 5B). These results demonstrate that the RRM domain of GRP162 possesses the ability to bind to *atp6-orfH79* RNA. The band-shifted complexes in Figures 5A and 5B migrate at a range of different sizes depending on the protein concentration, suggesting that either GRP162 binds to multiple sites on the probe or that GRP162 forms homodimers in vitro; this result also implies that GRP may bind to CMS-associated transcripts via two regions to form homodimers.

To determine which part of the *atp6-orfH79* mRNA sequence is recognized by GRP162, the intragenic *atp6-orfH79* mRNA was divided into three fragments, A, B, and C (Figure 2B). These fragments were further analyzed by EMSA. Fragments A and C displayed mobility shifts with GRP162, whereas fragment B did

not (Figure 5C). These observations suggest that GRP162 binds fragments A and C, which is consistent with our previous speculation that GRP162 may form homodimers.

The truncated *atp6-orfH79* sequences were also studied in the yeast three-hybrid system. Again, GRP162 bound to fragments A and C but not B. These results were further confirmed by a β -galactosidase activity assay that suggested a strong interaction between GRP162 and intragenic fragments A and C (Figure 5D). A 3-amino-1,2,4-triazole competition assay further verified the A and C fragment binding sites for GRP162 (Figure 5E). The 3-AT results are consistent with the BiFC results, demonstrating GRP162 homodimer formation in vivo. These data indicate that GRP162 binds specifically to intragenic sequences of *atp6-orfH79* transcripts.

To assess the interaction between GRP162 and the target RNA in vivo, protein-RNA coimmunoprecipitation was performed. Mitochondrial extracts were obtained from the YTA line and its F1 hybrid, respectively, and an antiserum against GRP162 was used for coimmunoprecipitation. Following the coimmunoprecipitation, RNA was extracted from both the supernatant and the immunoprecipitated pellet for reverse transcription. RT-PCR was performed with *atp6* and *orfH79* primers, and the results showed that the transcripts from *atp6-orfH79* were enriched in the pellet of the F1 hybrid but not in the supernatant, whereas no obvious PCR product was detected in the CMS line (Figure 6A). The negative control, 26S rRNA, was present in trace amounts. Based on these results, we postulate that GRP162 binds to CMS-associated transcripts and provides the RNA substrate required for processing.

RF5 and the GRP162 Are Components of a Fertility Restoration Complex

To explore whether RFC exists in the F1 hybrids, we performed a coimmunoprecipitation assay with an anti-GRP162 antibody. The hybridization signal from coimmunoprecipitation pellets was detected by immunoblotting using an antiserum against RF5 (Figure 6B). The results of these assays indicate that RF5 and the GRP162 work together in F1 hybrid mitochondria, and they establish the existence of an RFC.

To confirm the presence and size of the RFC in F1 hybrids, Blue Native (BN)-PAGE analysis and size-exclusion chromatography were employed. Protein extracts from lysed mitochondria were used to isolate the RFC. These samples were subjected to BN-PAGE, Coomassie staining, and immunoblot analysis with antisera against GRP162 and RF5. Comparison with Coomassie blue staining revealed that the immunosignals were at the same molecular mass (400 to 500 kD) when GRP162 and RF5 antibodies were used for immunoblot analysis (Figures 6C and 6D). Similar results were obtained by size-exclusion chromatography. As standard samples, ferritin (440 kD, 880 kD as a dimer), catalase (220 kD), and BSA (68 kD) were also tested (Figure 6F) to establish a standard curve. Crude protein from F1 hybrid mitochondria was separated by size-exclusion chromatography. Elution fractions 1 to 22 were analyzed by immunoblotting using antibodies against RF5 and GRP162. The signal peaked in fractions 8 and 9, corresponding to a molecular mass of \sim 440 kD (Figure 6E). These results suggest that an RFC is present in F1

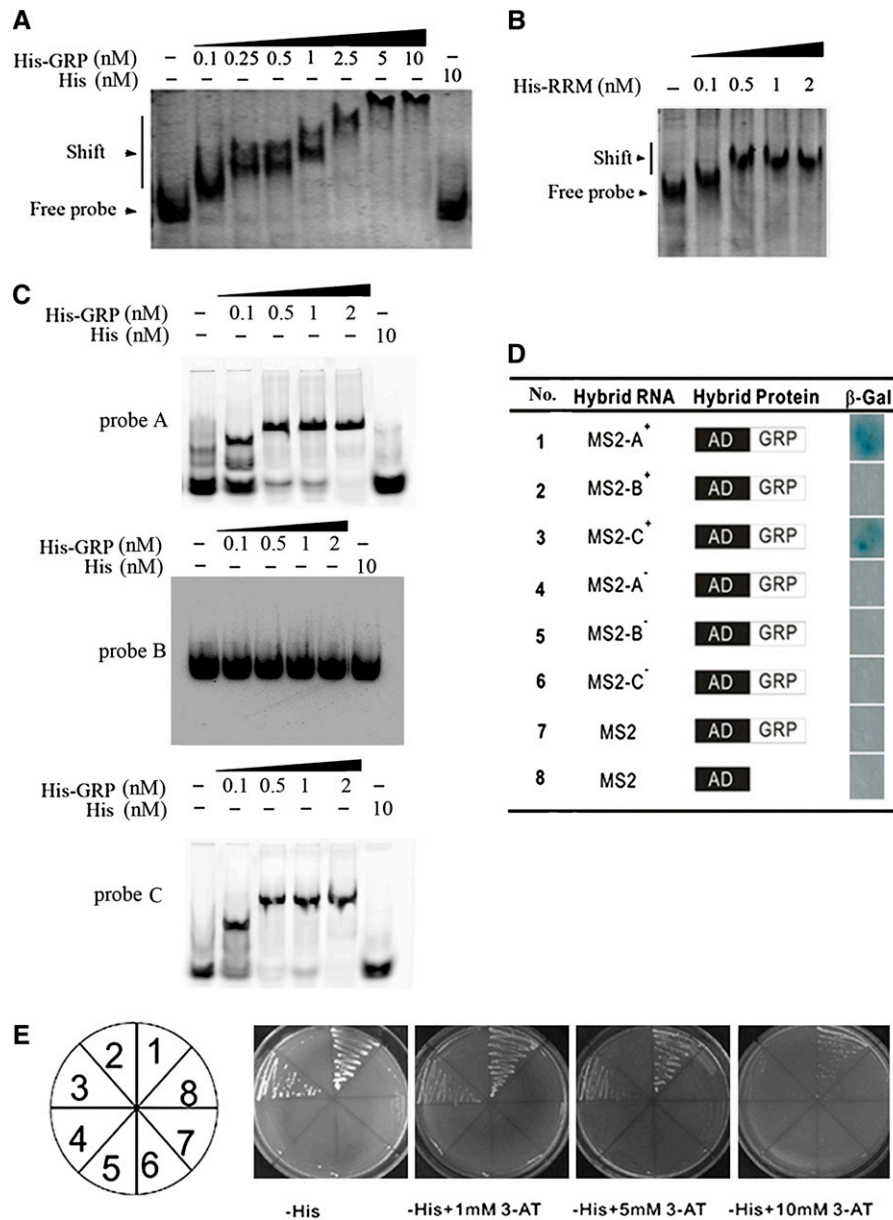


Figure 5. Interaction between the GRP162 and CMS-Associated Transcripts.

(A) EMSA of His-GRP162 and His-tag using a fixed concentration (0.5 nM) of the CMS RNA probe (diagrammed in Figure 2B) with a range of protein concentrations and His-tag as a control.

(B) EMSA of the His-tagged RRM domain of Rf5 (His-RRM) using a fixed concentration (0.5 nM) of the RNA probe (diagrammed in Figure 2B) with a range of protein concentrations.

(C) EMSAs with His-GRP162 and His-tag were performed using a fixed concentration (0.3 nM) of fragment A, B, or C as the RNA probe (diagrammed in Figure 2B) with a range of protein concentrations.

(D) β-Galactosidase activity for the three-hybrid assay and the details of rows 1 to 8. MS2-A⁺, MS2-B⁺, and MS2-C⁺ (indicated by A, B, and C, respectively) were ligated into pIII_{MS2-2} to produce sense strand RNA probes. MS2-A⁻, MS2-B⁻, and MS2-C⁻ denote reverse ligations that produce antisense strand RNA probes.

(E) After the transformants were selected for the presence of the plasmids, colonies were assayed for HIS3 reporter activity and 3-AT competition.

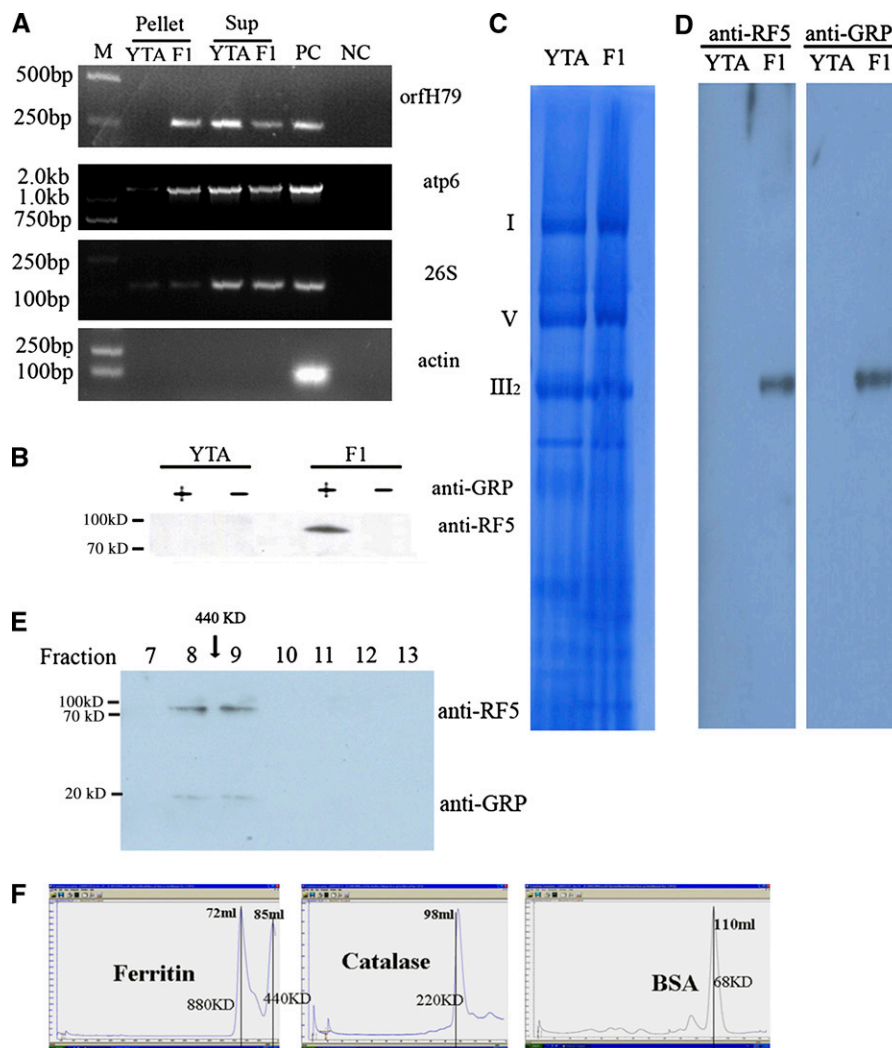


Figure 6. Identification of the RFC in Mitochondria.

(A) RT-PCR for *atp6* and *orfH79* to detect RNA-protein immunoprecipitates. Actin and 26S RNA were used as controls. cDNA was used as template in the positive control (PC), and RNA was used as template in the negative control (NC). M, marker DL2000.

(B) Coimmunoprecipitation assay with anti-GRP162 immunoprecipitates detected with anti-RF5 antibody.

(C) Coomassie blue staining of 100 μ g of mitochondria separated by native polyacrylamide gel electrophoresis. Complex I (I), Complex V (V), and Complex III₂ (III₂) are visible in the gel.

(D) Anti-RF5 and anti-GRP162 protein gel blots to detect the RF5 complex by BN-PAGE.

(E) Anti-RF5 and anti-GRP162 protein gel blots to detect F1 hybrid mitochondrial fractions resulting from size-exclusion chromatography with Superdex 200.

(F) Protein standards, including ferritin (440 kD, 880 kD as a dimer), catalase (220 kD), and BSA (68 kD), were run on Superdex 200.

[See online article for color version of this figure.]

hybrid mitochondria and that GRP162 and RF5 are components of this complex.

To assess RNA cleavage activity *in vitro*, we first investigated whether GRP162 and RF5, individually or in association, mediate RNA cleavage. Transcribed CMS RNA was incubated with recombinant RF5 and GRP162 proteins *in vitro*. The recombinant proteins were unable to cleave CMS-associated transcripts in mitochondria lysis buffer with additional ATP either individually or

together, suggesting that other unknown proteins in the RFC may participate in RNA cleavage (Figure 7A). To further investigate the RNA cleavage requirements, mitochondrial lysate from the CMS line was used as a substrate for incubation with additional RF5 and GRP162. RNA was extracted, reverse transcribed, and amplified by real-time quantitative PCR, confirming that the cleavage of CMS-associated RNA is dependent on additional mitochondrial components of the RFC (Figure 7B).

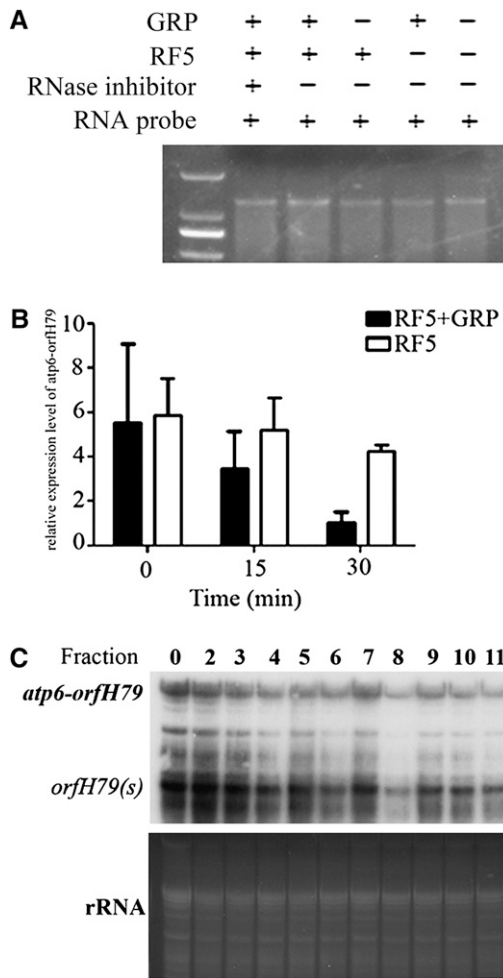


Figure 7. In Vitro Cleavage Activity Assay for RF5 and GRP162.

(A) Transcribed RNAs encompassing the intragenic region of *atp6-orfH79* from 19 to 1285 nucleotides were incubated in vitro with recombinant RF5 and GRP162 to assess cleavage activity.

(B) An RNA cleavage assay using RNA and protein from mitochondrial extract from the HL-CMS line together with recombinant RF5 and GRP162. Reverse transcription for time-dependent quantitative PCR analysis of the expression of *atp6-orfH79*. The vertical line (the y axis) corresponds to the relative transcript level, and each bar represents the mean \pm SD ($n = 3$).

(C) An RNA cleavage assay with total mitochondrial RNA as substrate for fractions 2 to 11 from the size-exclusion chromatography and with PBS as the control in fraction 0 (line 1). The RNA was analyzed by RNA gel blotting with *orfH79* as a probe.

Size-exclusion chromatography fractions were subsequently used to evaluate RNA cleavage activity, and total RNA from the CMS line was incubated with these fractions. RNA gel blot analysis with *orfH79* as a probe established that the CMS-associated transcripts were cleaved by fraction 8 (Figure 7C).

These results suggest that GRP162 interacts with RF5 and other unknown components in a complex that mediates the cleavage of CMS-associated RNAs. Our results suggest that

both GRP162 and RF5 are essential for the RNA processing associated with fertility restoration.

GRP162 Silencing Impairs RFC Activity

To more fully characterize the biological role of GRP162 in the CMS/*Rf* pathway, we suppressed the expression of *GRP162* by RNA interference (RNAi). The RNAi construct was transformed into calli induced from the mature seeds of restorer line *Rf5*(NIL), and a total of 13 T0 transformant lines expressing *GRP162i* were obtained. Quantitative RT-PCR results showed that three of the 13 lines displayed greatly reduced expression of *GRP162* (Figure 8A); these were designated GRPi-1, GRPi-2, and GRPi-3.

We next examined the expression of CMS-associated transcripts in the three RNAi lines by RNA gel blot analysis, focusing on the processing of *atp6-orfH79*. The 2.0-kb transcript of *atp6-orfH79* was detected in the CMS line YTA calli and transgenic calli but not in the restorer line *Rf5*(NIL) calli (Figure 8B). These results suggest that the processing activity of RFC is impaired in the RNAi lines, leading to the accumulation of the

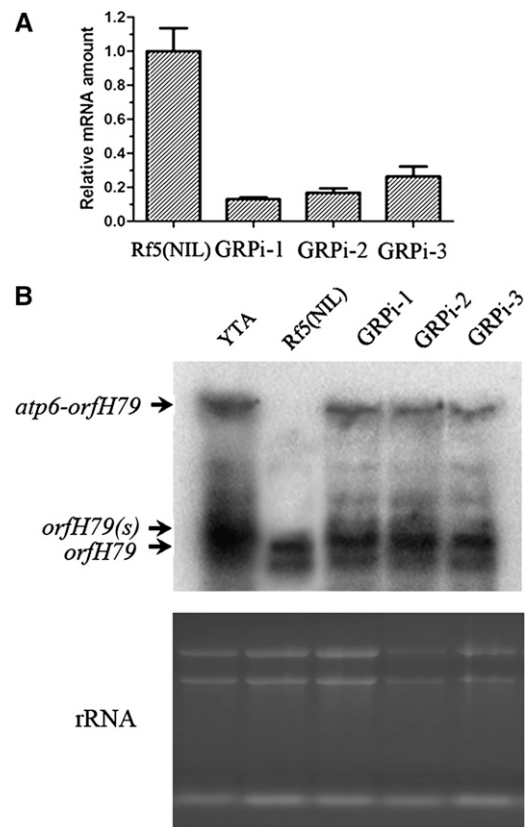


Figure 8. Analysis of GRP RNAi Lines.

(A) Quantitative RT-PCR analysis of GRP162 expression levels in *Rf5*(NIL) and GRP-RNAi lines. The data are shown as mean \pm SD ($n = 3$).

(B) RNA gel blot analysis of the CMS-associated transcript *atp6-orfH79* in the YTA, *Rf5*(NIL), and GRP-RNAi lines. Ethidium bromide staining of the gel confirms equal RNA loading.

GRP162, which lacks a mitochondrial presequence, appears to be a cytosolic protein that localizes to mitochondria in association with RF5. We speculate two possibilities to account for this observation. In one scenario, GRP162 is expressed constitutively in the cytoplasm of *rf/rf* lines, and RF5 serves to recruit GRP162 into mitochondria in F1 hybrid plants. Alternatively, GRP162 protein may enter mitochondria in *rf/rf* lines in only trace amounts, perhaps because it is degraded in the absence of RF5 as a stabilizing interactor. Both explanations warrant further investigation. The elevated expression of GRP162 may be another reason for its altered localization in the presence of *Rf5*. The constitutive expression of GRP162 in the *rf/rf* background suggests that it likely performs additional, still undetermined, biological functions. Our results indicate that PPR791 interacts with GRP162 both in vitro and in vivo, with the GRP protein appearing to be indispensable for *atp6-orfH79* mRNA processing.

Primer extension assays indicate that the processing site within the *atp6-orfH79* transcript is 1169 nucleotides away from the *Atp6* start codon (Figure 9A), and the processing site does not appear to pair with other regions of the transcript according to secondary structure predictions (Figure 9B). Thus, GRP162 appears to function as a homodimer that bind regions A and C of the *atp6-orfH79* transcript, likely forming a hairpin loop structure that may serve as a substrate for RNA processing. Additional components are predicted to participate in the RFC, and it remains to be determined which factor possesses an endoribonuclease for RNA processing activity. The results of this study bring us closer to answering these questions.

METHODS

Materials for Fine Mapping

An *Rf5* NIL (denoted NIL) was obtained by repeated backcrossing to the CMS line, YTA, for several generations with the restorer line Milyang23. YueTai B (*rf5/rf5*) is a male-fertile maintainer line used as the male parent for propagation of YTA and has the same nuclear genomic DNA but different mitochondrial DNA. A BC₈F₁ population containing 1979 individuals resulted from a cross of YTA/NIL/YTB. SSR primers were used for the fine mapping of *Rf5*, which is located on chromosome 10.

RNA Extraction, RT-PCR, and RNA Gel Blot Analysis

Total RNA was isolated with TRIzol reagent (Invitrogen). Approximately 4 µg of RNA was treated with DNase I (NEB), and cDNA was obtained by reverse transcription with SuperScriptII as described in the manufacturer's instructions. Real-time quantitative PCR was performed with the LightCycler 480 (Roche) and the SYBR Green I Master PCR kit (Roche). GRP162 was amplified in YTA and NILF₁ to detect the relative expression, respectively. *atp6-orfH79* and *orfH79* were amplified using the primers listed in Supplemental Table 5 online. Approximately 20 µg of total RNA was used for RNA gel blots with *orfH79* as a probe. A random-primer DNA labeling kit (Takara) was used for hybridization.

Screening a BAC Library for the *Rf5* Locus, Subcloning, and Sequencing

High-density filters from a Milyang23 genomic BAC library for colony hybridization were a gift from the Korean Agricultural Culture Collection. A BAC clone covering the *Rf5* locus (17E08) was purchased from the

J. Craig Venter Institute and used for probe preparation. The positive BAC clone (68F6) was digested with *Sall* for subcloning into pUC18, and sequencing was performed by the National Center for Gene Research, Chinese Academy of Sciences.

Complementation Tests for *Rf5* Candidate Genes

The *Rf5* candidate genes were obtained by PCR amplification using the 68F6 BAC clone as a template. The PCR products were ligated into the *Bam*HI site of the pCAMBIA1301-UBI binary vector with expression driven by the ubiquitin promoter (Chen et al., 2007) and introduced into the CMS line YTA (*Oryza sativa* subsp *indica*) by *Agrobacterium tumefaciens*-mediated transformation. Pollen fertility was the phenotype used to identify the transgenic plants. The fertility restoration phenotype was tested with potassium iodide (1% I₂-KI) staining and seed setting.

Construction and Screening of the Bacterial Two-Hybrid Library

A cDNA library from an F1 spikelet was constructed with the Bacterio-Match II Two-Hybrid System Library Construction kit (Stratagene) according to the manufacturer's instructions. To screen for partner proteins, the transit peptide of RF5 was removed and the remaining sequence was ligated into the *Bam*HI site of pBT as bait. The screening and validation of positive clones was performed according to the manufacturer's instructions. Bioinformatic analysis of the sequencing data from the positive clones was performed using BLAST at the NCBI database website.

Validation with the Yeast Two-Hybrid System

The GRP162 cDNA was ligated into pGADT7 and sequenced, and *Rf5* was cloned into the pGBKT7 *Bam*HI site. Competent yeast cells were prepared according to a standard protocol (Wu and Letchworth, 2004). The constructs were cotransformed into the AH109 yeast strain in pairs, and the transformants were plated on SD/-Leu/-Trp medium and incubated at 30°C for 3 d, picked and grown on SD/-Leu/-Trp/-His plates at 30°C for 3 d, and then cultured on SD/-Leu/-Trp/-His/-Ade plates for 3 d.

In Vivo Interaction by BiFC Assay

For the BiFC studies, full-length cDNA was amplified from both the candidate partner proteins and RF5 and fused to either an N- or C-terminal fragment of YFP in pUC-SPYNE (N-terminal) or pUC-SPYNE (C-terminal), respectively (Walter et al., 2004). The two vectors were cotransformed into onion epidermal cells in pairs using particle bombardment. For transient expression, all the constructs were fully sequenced, and particle bombardment was performed using onion cells as follows. Gold particles (1.0 µm in diameter) were washed with 100% ethanol and coated with 20 µg of each DNA. The DNA-coated gold particles were projected using a Bio-Rad PDS1000/He particle gun. Tissues were bombarded at a helium pressure of 1100 p.s.i., and the distance between the target tissue and rupture disc was 10 cm. Following particle bombardment, the tissues were incubated in the dark at 27°C for 16 to 20 h after bombardment on Murashige and Skoog medium. The cell layers were then stained with MitoTracker Red (Invitrogen) for 20 min and washed with PBS three times and finally mounted in water and examined via bright-field and fluorescent microscopy using a Leica DM4000B microscope.

The Expression of rRF5, rGRP162, and rRRM in *E. coli*

The *Rf5* sequence corresponding to the putative mature protein was amplified and ligated into pMAL-c2x (NEB), and the recombinant MBP-RF5 protein was purified with an amylose column. The full-length cDNAs

of the GRP162 and RRM segments were amplified by PCR (using primers designed according to their database sequences; see Supplemental Table 5 online) and then sequenced. These fragments were inserted into pET32a for expression (Novagen). The His-GRP162, His-RRM, and His-tag recombinant proteins were purified with a HisTrap FF column (GE Healthcare). The concentrations of the proteins were determined with a modified Lowry protein assay kit (Thermo Scientific). Prior to their use in the RNA assay, the proteins were dialyzed against a buffer consisting of 10 mM HEPES, pH 7.0, 100 mM KCl, and 5 mM MgCl₂.

Pull-Down Assay

All the following procedures were performed with the AKTA Prime plus protein purification system (GE Healthcare). His-GRP162 was injected onto a His-Trap FF column, and the column was washed with 10 volumes of PBS, pH 7.4. After the MBP-RF5 was injected, the column was washed with an additional 10 volumes of PBS, pH 7.4. Finally, the binding proteins were eluted with 300 mM imidazole. All fractions were subjected to 10% SDS-PAGE with Coomassie blue staining. Elution fraction 9 was subjected to immunoblotting with anti-His and anti-MBP antibodies. For the control assays, the His-tag and MBP-tag expressed from the pET32a and pMALc2x empty vectors were separately loaded onto His-Trap and amylose columns, respectively. After the columns were equilibrated with 10 volumes of PBS, the MBP-RF5 and His-GRP162 recombinant proteins were loaded onto the reciprocal columns to detect any false positive interactions caused by the fused tag.

EMSAs

Using PCR-amplified fragments of *atp6-orfH79* as templates, RNA probes for the EMSA were transcribed in vitro via a T7 promoter at the 5' end. The fragments were amplified using the primer pairs RNApF and RNApR. The RNA probe was gel purified, the 5' end was labeled with T4 polynucleotide kinase and [³²P]ATP, and the probe was purified by ethanol precipitation. For the EMSA, various quantities of purified recombinant GRP162 were incubated with labeled RNA probe in a 20- μ L reaction mixture including 10 μ L of 2 \times binding buffer (100 mM Na phosphate, pH 7.5, 10 units RNasin, 0.1 mg/mL BSA, 10 mM DTT, 2.5 mg/mL heparin, and 300 mM NaCl). Yeast tRNA was used as a negative control. The mixture was incubated at 25°C for 30 min. The samples were separated by 5% native PAGE in 0.5 \times TBE buffer and then exposed to a phosphor imager screen and analyzed on a Typhoon 9200 instrument (GE Healthcare).

The Yeast Three-Hybrid System as an RNA Binding Assay

The yeast strain YBZ-1 was used in yeast three-hybrid assays according to standard protocols (Bernstein et al., 2002). The *Rf5* sequence corresponding to the putative protein and the full sequence of GRP162 were amplified with *Rf5*-Y3F and *Rf5*-Y3R or GRP162-Y3F and GRP162-Y3R, respectively. The fragments were ligated into pACT11 to construct the hybrid protein vectors. The *atp6-orfH79* intragenic region was divided into fragments A, B, and C, which were amplified using three pairs of primers, AF and AR, BF and BR, and CF and CR (see Supplemental Table 5 online). The fragments were ligated into pIII/MS2-2 to construct the hybrid RNA vectors. The fusion protein vectors and the hybrid RNA vectors were then cotransformed into YBZ-1, and positive clones were selected on medium containing SD/-Leu/-Ura. These recombinant yeast clones were cultured for 2 d at 28°C and scored on SD/-His plates with either 0, 1, 5, or 10 mM 3-AT. After a 3-d culture at 28°C, interactions were observed. In addition, β -galactosidase activity was measured in standard filter assays using X-Gal as the chromogenic substrate.

Coimmunoprecipitation

All mitochondria used in this study were isolated from etiolated seedlings cultured in the dark for 1 week at 30°C. Crude mitochondria were purified as described elsewhere (Heazlewood et al., 2003). A 19-amino acid peptide was synthesized by NewEast Biosciences and used for the preparation of anti-GRP162 serum (see Supplemental Figure 8 online). The anti-RF5 serum was prepared with the recombinant MBP-RF5 protein. Coimmunoprecipitation was performed as previously described (Uyttewaal et al., 2008). One milligram of crude mitochondria from YTA and the F1 hybrid etiolated seedlings was lysed in modified mitochondrial lysis buffer (10 mM HEPES, pH 7.0, 100 mM KCl, 5 mM MgCl₂, 0.5% Nonidet P-40, and a protease inhibitor cocktail [Roche]). The cell lysates were incubated with rabbit anti-GRP162 serum on ice for 5 h. After the addition of 50 μ L of protein A/G beads, the lysates were incubated on ice overnight with gentle shaking. The beads were washed with PBS buffer four times while on ice. The RNA was extracted from the coimmunoprecipitation pellets, and the supernatants were reverse transcribed with SuperScript II using random primers to obtain cDNA for RT-PCR. The proteins for the immunoblots were eluted in 1 \times SDS running buffer by heating at 95°C for 5 min.

Mitochondrial Protein Immunoblots

Twenty micrograms of protein was fractionated by SDS-PAGE, electrotransferred to a polyvinylidene fluoride transfer membrane (GE Healthcare), and hybridized with polyclonal antibodies to the GRP162 protein (1:2000). Anti-RPL12 antibodies (1:2000) were used as a positive control, and antitubulin antibodies (1:2000) were used as a negative control. Horseradish peroxidase-linked secondary antibodies (mouse anti-rabbit or goat anti-mouse) and the ECL Plus reagent were used for visualization (Thermo Scientific).

BN-PAGE and Size-Exclusion Chromatography

The crude mitochondrial proteins from YTA and the F1 hybrid (100 μ g each) were extracted with MLB and loaded onto BN-PAGE as described (Wittig et al., 2006). The proteins were visualized by Coomassie Brilliant Blue staining and immunoblotting with anti-RF5 and anti-GRP162 sera. The supernatant from the F1 hybrid mitochondria was loaded onto a 120-cm column with Superdex 200 (GE Healthcare). The standard samples, ferritin (440 kD, 880 kD as a dimer), catalase (220 kD), and BSA (68 kD), were first run on Superdex 200. The mitochondria samples treated with RNase A were then treated with 200 units of RNase inhibitor (NEB) during lysis for size exclusion chromatography. Fractions of \sim 1.5 mL were sequentially collected from the column. The samples were used for SDS-PAGE and immunoblotting with anti-RF5 and anti-GRP162 sera.

RNA Cleavage Activity Assay

Mitochondrial RNA from the CMS line was incubated with recombinant proteins or size-exclusion chromatography fractions for 30 min at 37°C and then extracted with trichloromethane twice for loading. For substrate, mitochondria from the CMS line were lysed in modified MLB, and recombinant proteins were added to detect whether the CMS-associated transcripts can be cleaved. The RNA gel blot analysis used *orfH79* as a probe.

Primer Extension Assay

To determine the RNA processing site of *atp6-orfH79*, a primer extension assay was performed according to a standard protocol (Kazama et al., 2008). The secondary structure of *atp6-orfH79* was predicted using RNAdraw 1.1 software (<http://www.rnadrw.com/>).

In Vivo Silencing of GRP162

GRP162 sequences (ranging from 240 to 439 bp) used in the in vivo silencing experiments were amplified from the full-length cDNA fragment and cloned into the pH7GWIWG(II) vector (Karimi et al., 2002) to produce double-stranded RNA. Calli induced from NIL seeds were used for *Agrobacterium*-mediated transformation. Calli of the RNAi lines were selected on Murashige and Skoog medium containing 50 mg/L hygromycin B.

Accession Numbers

Sequence data from this article for the cDNA of *Rf5* and GRP162 can be found in the GenBank/EMBL data libraries under accession numbers AB179840 and AK289192, respectively.

Supplemental Data

The following materials are available in the online version of this article.

Supplemental Figure 1. *rf5* in HL-CMS Line YTA.

Supplemental Figure 2. The Sequences of *atp6-orfH79*.

Supplemental Figure 3. Expression and Verification of MBP-RF5.

Supplemental Figure 4. Yeast Three-Hybrid System for Detecting the Interaction between RF5 and Intragenic Fragments of CMS-Associated Transcripts.

Supplemental Figure 5. Investigation of the Length of Bacterio-MatchII Two-Hybrid Library.

Supplemental Figure 6. The Expression of GRP162.

Supplemental Figure 7. The Expression and Purification of His-GRP and His-RRM.

Supplemental Figure 8. Sequences of a Gly-Rich Protein.

Supplemental Table 1. Pollen Fertility of T0 Transgenics (Stained with 1% I₂-KI).

Supplemental Table 2. Pollen Fertility of T1 of *PPR791* Transgenics (Stained with 1% I₂-KI).

Supplemental Table 3. Pollen Fertility of F1 Progeny with the *PPR791* T0 Plant Backcrossed to YTA (Stained with 1% I₂-KI).

Supplemental Table 4. The Candidate Partner Proteins of RF5.

Supplemental Table 5. Primers Used in This Study.

ACKNOWLEDGMENTS

We thank Yong-Hwan Kim and Ung-Han Yoon for kindly providing the Milyang23 BAC library, Marvin Wickens for providing the yeast three-hybrid system, and Hakim Mireau for providing the anti-RPL12 antibody. We also thank Sally A. Mackenzie and Qifa Zhang for critical comments on the manuscript. This work was supported by funds from the National Basic Research Program of China (2007CB109005), the Creative Research Group of the National Natural Science Foundation of China (30821064), and the National High-Tech Research and Development Project (2009AA101101).

AUTHOR CONTRIBUTIONS

J.H., D.Y., and Y.Z. designed the research. J.H., K.W., W.H., G.L., Y.G., J.W., Q.H., X.Q., Y.J., L.W., and R.Z. performed research. J.H., K.W., W.H., S.L., D.Y., and Y.Z. analyzed data. J.H., W.H., and D.Y. wrote the article.

Received November 2, 2011; revised November 2, 2011; accepted December 27, 2011; published January 13, 2012.

REFERENCES

- Akagi, H., Nakamura, A., Yokozeki-Misono, Y., Inagaki, A., Takahashi, H., Mori, K., and Fujimura, T. (2004). Positional cloning of the rice *Rf-1* gene, a restorer of BT-type cytoplasmic male sterility that encodes a mitochondria-targeting PPR protein. *Theor. Appl. Genet.* **108**: 1449–1457.
- Beick, S., Schmitz-Linneweber, C., Williams-Carrier, R., Jensen, B., and Barkan, A. (2008). The pentatricopeptide repeat protein PPR5 stabilizes a specific tRNA precursor in maize chloroplasts. *Mol. Cell. Biol.* **28**: 5337–5347.
- Bentolila, S., Alfonso, A.A., and Hanson, M.R. (2002). A pentatricopeptide repeat-containing gene restores fertility to cytoplasmic male-sterile plants. *Proc. Natl. Acad. Sci. USA* **99**: 10887–10892.
- Bernstein, D.S., Buter, N., Stumpf, C., and Wickens, M. (2002). Analyzing mRNA-protein complexes using a yeast three-hybrid system. *Methods* **26**: 123–141.
- Brown, G.G., Formanová, N., Jin, H., Wargachuk, R., Dendy, C., Patil, P., Laforest, M., Zhang, J., Cheung, W.Y., and Landry, B.S. (2003). The radish *Rfo* restorer gene of Ogura cytoplasmic male sterility encodes a protein with multiple pentatricopeptide repeats. *Plant J.* **35**: 262–272.
- Chase, C.D. (2007). Cytoplasmic male sterility: A window to the world of plant mitochondrial-nuclear interactions. *Trends Genet.* **23**: 81–90.
- Chen, R., Zhao, X., Shao, Z., Wei, Z., Wang, Y., Zhu, L., Zhao, J., Sun, M., He, R., and He, G. (2007). Rice UDP-glucose pyrophosphorylase1 is essential for pollen callose deposition and its cosuppression results in a new type of thermosensitive genic male sterility. *Plant Cell* **19**: 847–861.
- Cui, X., Wise, R.P., and Schnable, P.S. (1996). The *rf2* nuclear restorer gene of male-sterile T-cytoplasm maize. *Science* **272**: 1334–1336.
- Delannoy, E., Stanley, W.A., Bond, C.S., and Small, I.D. (2007). Pentatricopeptide repeat (PPR) proteins as sequence-specificity factors in post-transcriptional processes in organelles. *Biochem. Soc. Trans.* **35**: 1643–1647.
- Desloire, S., et al. (2003). Identification of the fertility restoration locus, *Rfo*, in radish, as a member of the pentatricopeptide-repeat protein family. *EMBO Rep.* **4**: 588–594.
- Dollins, D.E., Warren, J.J., Immormino, R.M., and Gewirth, D.T. (2007). Structures of GRP94-nucleotide complexes reveal mechanistic differences between the hsp90 chaperones. *Mol. Cell* **28**: 41–56.
- Fujii, S., and Toriyama, K. (2009). Suppressed expression of Retrograde-Regulated Male Sterility restores pollen fertility in cytoplasmic male sterile rice plants. *Proc. Natl. Acad. Sci. USA* **106**: 9513–9518.
- Gillman, J.D., Bentolila, S., and Hanson, M.R. (2007). The petunia restorer of fertility protein is part of a large mitochondrial complex that interacts with transcripts of the CMS-associated locus. *Plant J.* **49**: 217–227.
- Hanson, M.R., and Bentolila, S. (2004). Interactions of mitochondrial and nuclear genes that affect male gametophyte development. *Plant Cell* **16** (suppl.): S154–S169.
- Heazlewood, J.L., Howell, K.A., Whelan, J., and Millar, A.H. (2003). Towards an analysis of the rice mitochondrial proteome. *Plant Physiol.* **132**: 230–242.
- Itabashi, E., Iwata, N., Fujii, S., Kazama, T., and Toriyama, K. (2011). The fertility restorer gene, *Rf2*, for Lead Rice-type cytoplasmic male sterility of rice encodes a mitochondrial glycine-rich protein. *Plant J.* **65**: 359–367.
- Itabashi, E., Kazama, T., and Toriyama, K. (2009). Characterization of

- cytoplasmic male sterility of rice with Lead Rice cytoplasm in comparison with that with Chinsurah Boro II cytoplasm. *Plant Cell Rep.* **28**: 233–239.
- Karimi, M., Inzé, D., and Depicker, A.** (2002). GATEWAY vectors for Agrobacterium-mediated plant transformation. *Trends Plant Sci.* **7**: 193–195.
- Kazama, T., Nakamura, T., Watanabe, M., Sugita, M., and Toriyama, K.** (2008). Suppression mechanism of mitochondrial ORF79 accumulation by Rf1 protein in BT-type cytoplasmic male sterile rice. *Plant J.* **55**: 619–628.
- Kazama, T., and Toriyama, K.** (2003). A pentatricopeptide repeat-containing gene that promotes the processing of aberrant atp6 RNA of cytoplasmic male-sterile rice. *FEBS Lett.* **544**: 99–102.
- Klein, R.R., Klein, P.E., Mullet, J.E., Minx, P., Rooney, W.L., and Schertz, K.F.** (2005). Fertility restorer locus Rf1 [corrected] of sorghum (*Sorghum bicolor* L.) encodes a pentatricopeptide repeat protein not present in the colinear region of rice chromosome 12. *Theor. Appl. Genet.* **111**: 994–1012.
- Koizuka, N., Imai, R., Fujimoto, H., Hayakawa, T., Kimura, Y., Kohno-Murase, J., Sakai, T., Kawasaki, S., and Imamura, J.** (2003). Genetic characterization of a pentatricopeptide repeat protein gene, orf687, that restores fertility in the cytoplasmic male-sterile Kosenia radish. *Plant J.* **34**: 407–415.
- Komori, T., Ohta, S., Murai, N., Takakura, Y., Kuraya, Y., Suzuki, S., Hiei, Y., Imaseki, H., and Nitta, N.** (2004). Map-based cloning of a fertility restorer gene, Rf-1, in rice (*Oryza sativa* L.). *Plant J.* **37**: 315–325.
- Kotera, E., Tasaka, M., and Shikanai, T.** (2005). A pentatricopeptide repeat protein is essential for RNA editing in chloroplasts. *Nature* **433**: 326–330.
- Liu, X.Q., Xu, X., Tan, Y.P., Li, S.Q., Hu, J., Huang, J.Y., Yang, D.C., Li, Y.S., and Zhu, Y.G.** (2004). Inheritance and molecular mapping of two fertility-restoring loci for Honglian gametophytic cytoplasmic male sterility in rice (*Oryza sativa* L.). *Mol. Genet. Genomics* **271**: 586–594.
- Maris, C., Dominguez, C., and Allain, F.H.** (2005). The RNA recognition motif, a plastic RNA-binding platform to regulate post-transcriptional gene expression. *FEBS J.* **272**: 2118–2131.
- Okuda, K., Chateigner-Boutin, A.L., Nakamura, T., Delannoy, E., Sugita, M., Myouga, F., Motohashi, R., Shinozaki, K., Small, I., and Shikanai, T.** (2009). Pentatricopeptide repeat proteins with the DYW motif have distinct molecular functions in RNA editing and RNA cleavage in *Arabidopsis* chloroplasts. *Plant Cell* **21**: 146–156.
- Okuda, K., Nakamura, T., Sugita, M., Shimizu, T., and Shikanai, T.** (2006). A pentatricopeptide repeat protein is a site recognition factor in chloroplast RNA editing. *J. Biol. Chem.* **281**: 37661–37667.
- Peng, X., Wang, K., Hu, C., Zhu, Y., Wang, T., Yang, J., Tong, J., Li, S., and Zhu, Y.** (2010). The mitochondrial gene orfH79 plays a critical role in impairing both male gametophyte development and root growth in CMS-Honglian rice. *BMC Plant Biol.* **10**: 125.
- Pfalz, J., Bayraktar, O.A., Prikryl, J., and Barkan, A.** (2009). Site-specific binding of a PPR protein defines and stabilizes 5' and 3' mRNA termini in chloroplasts. *EMBO J.* **28**: 2042–2052.
- Pfalz, J., Liere, K., Kandlbinder, A., Dietz, K.J., and Oelmüller, R.** (2006). pTAC2, -6, and -12 are components of the transcriptionally active plastid chromosome that are required for plastid gene expression. *Plant Cell* **18**: 176–197.
- Robbins, J.C., Heller, W.P., and Hanson, M.R.** (2009). A comparative genomics approach identifies a PPR-DYW protein that is essential for C-to-U editing of the *Arabidopsis* chloroplast accD transcript. *RNA* **15**: 1142–1153.
- Salone, V., Rüdinger, M., Polsakiewicz, M., Hoffmann, B., Groth-Malonek, M., Szurek, B., Small, I., Knoop, V., and Lurin, C.** (2007). A hypothesis on the identification of the editing enzyme in plant organelles. *FEBS Lett.* **581**: 4132–4138.
- Schmitz-Linneweber, C., and Small, I.** (2008). Pentatricopeptide repeat proteins: A socket set for organelle gene expression. *Trends Plant Sci.* **13**: 663–670.
- Schmitz-Linneweber, C., Williams-Carrier, R., and Barkan, A.** (2005). RNA immunoprecipitation and microarray analysis show a chloroplast pentatricopeptide repeat protein to be associated with the 5' region of mRNAs whose translation it activates. *Plant Cell* **17**: 2791–2804.
- Schmitz-Linneweber, C., Williams-Carrier, R.E., Williams-Voelker, P.M., Kroeger, T.S., Vichas, A., and Barkan, A.** (2006). A pentatricopeptide repeat protein facilitates the trans-splicing of the maize chloroplast rps12 pre-mRNA. *Plant Cell* **18**: 2650–2663.
- Shikanai, T.** (2006). RNA editing in plant organelles: Machinery, physiological function and evolution. *Cell. Mol. Life Sci.* **63**: 698–708.
- Uyttewaal, M., Arnal, N., Quadrado, M., Martin-Canadell, A., Vrielynck, N., Hiard, S., Gherbi, H., Bendahmane, A., Budar, F., and Mireau, H.** (2008). Characterization of *Raphanus sativus* pentatricopeptide repeat proteins encoded by the fertility restorer locus for Ogura cytoplasmic male sterility. *Plant Cell* **20**: 3331–3345.
- Vermel, M., Guermann, B., Delage, L., Grienberger, J.M., Maréchal-Drouard, L., and Gualberto, J.M.** (2002). A family of RRM-type RNA-binding proteins specific to plant mitochondria. *Proc. Natl. Acad. Sci. USA* **99**: 5866–5871.
- Walter, M., Chaban, C., Schütze, K., Batistic, O., Weckermann, K., Näge, C., Blazevic, D., Grefen, C., Schumacher, K., Oecking, C., Harter, K., and Kudla, J.** (2004). Visualization of protein interactions in living plant cells using bimolecular fluorescence complementation. *Plant J.* **40**: 428–438.
- Wang, Z., et al.** (2006). Cytoplasmic male sterility of rice with boro II cytoplasm is caused by a cytotoxic peptide and is restored by two related PPR motif genes via distinct modes of mRNA silencing. *Plant Cell* **18**: 676–687.
- Williams, P.M., and Barkan, A.** (2003). A chloroplast-localized PPR protein required for plastid ribosome accumulation. *Plant J.* **36**: 675–686.
- Wittig, I., Braun, H.P., and Schägger, H.** (2006). Blue native PAGE. *Nat. Protoc.* **1**: 418–428.
- Wu, S., and Letchworth, G.J.** (2004). High efficiency transformation by electroporation of *Pichia pastoris* pretreated with lithium acetate and dithiothreitol. *Biotechniques* **36**: 152–154.
- Yi, P., Wang, L., Sun, Q.P., and Zhu, Y.G.** (2002). Discovery of mitochondrial chimeric gene associated with cytoplasmic male sterility of HL rice. *Chin. Sci. Bull.* **47**: 744–747.
- Zaltsman, Y., et al.** (2010). MTCH2/MIMP is a major facilitator of tBID recruitment to mitochondria. *Nat. Cell Biol.* **12**: 553–562.
- Zamora, M., Meroño, C., Viñas, O., and Mampel, T.** (2004). Recruitment of NF-kappaB into mitochondria is involved in adenine nucleotide translocase 1 (ANT1)-induced apoptosis. *J. Biol. Chem.* **279**: 38415–38423.